[10]See R. H. Rogers, Rep. Prog. Phys. 39, 1 (1976).

[11]As Eq. (3) shows, since electric fields are screened their effect on a Coulomb fluid is different from the normal buoyancy forces.

[12]One should note the similarities and discrepances between this secular equation and that obtained by D. K. Moore and N. O. Weiss, J. Fluid Mech. 58, 289 (1973), in their analysis of the thermohaline problem.

[13]See, for instance, David H. Sattinger, *Topics in Stability and Bifurcation Theory* (Springer, Berlin, 1973), and, for the double-diffusive problem, H. E. Huppert, Nature 263, 20 (1976).

Solid-State Nuclear Spin-Flip Maser Pumped by Dynamic Nuclear Polarization

P. Bösiger, E. Brun, and D. Meier
Physik-Institut, Universität Zürich, Zürich, Switzerland
(Received 20 December 1976)

We report the observation of a coherent, maser-type rf radiation of the ^{27}Al nuclear-spin system in $Al_2O_3:Cr^{3+}$ pumped by dynamic nuclear polarization to negative temperature. A theoretical description is presented for the sharp, superradiant bursts which follow the fast tuning of a resonant LC circuit to a selected NMR line of ^{27}Al. Experimental results are discussed which demonstrate the interplay between dynamic nuclear polarization, relaxation, and the radiation field.

In diamagnetic crystals doped with paramagnetic centers, large nuclear-spin polarizations can be obtained by dynamic nuclear polarization (DNP). For an inverted magnetization a coherent maser-type NMR signal[1-3] is anticipated under favorable conditions. In this Letter, we wish to report the direct observation of coherently radiated nuclear-spin energy from ^{27}Al in Al_2O_3 into an LC circuit and to give a quantitative explanation of the superradiant bursts which precede the continuous maser-type spin oscillations. In particular, we would like to demonstrate that the pattern of the transient maser radiation reflects some important properties of the spin dynamics leading to DNP and to nuclear-spin relaxation.

For the experiments a single crystal of ruby $Al_2O_3:Cr^{3+}$ with a chromium concentration of nominally 0.013% was selected. A thirteen-turn coil was wound directly onto a roughly cylindrical specimen of 0.4 cm radius and 1.2 cm length. The sample was placed inside a multimode cavity and oriented such that the two ESR transitions between the lowest Cr^{3+} states coincided.[4] The magnetic field was 11.24 kG and the lattice temperature was 1.6 K. The coil was connected to an external capacitor which had a small Varicap in parallel, thus forming a resonant rf circuit with a Q of 40. The electrically controlled capacitor could be used for fast tuning. Effectively, it was acting as a Q switch. The probe of a HP-183 A oscilloscope was directly connected to the tuning capacitor.

Because of a small electric quadrupole interaction, the NMR spectrum of the bulk ^{27}Al is split into five well-separated lines. In a maser oscillation only those spins participate which populate neighboring Zeeman states, and to which the LC circuit is tuned. Thus the maser-active spins form a two-level system of fictitious spin-$\frac{1}{2}$ particles.[5] The analysis of our system can be based on a model which was first formulated by Bloembergen and Pound[6] and used by others[7,8] to explain the origin of the modulation pattern in two-level maser experiments.

The dynamical behavior of the system depends strongly on various time constants: the circuit ringing time $T_c = 2Q/\omega_c$, where $\omega_c = (LC)^{-1/2}$; the radiation damping time T_R; the spin dephasing time T_2; the DNP pumping time T_p; the spin-lattice relaxation time T_1; and, in particular, the characteristic time $T_{ss,\mathrm{Al}}$ for the coupling of the two-level system to the electronic interaction system. This coupling makes a rather fast transfer of spin energy between the different two-level systems of ^{27}Al via the electronic dipole-dipole reservoir possible. The experimental values are 10^{-6}, 3×10^{-5}, ~65, and ~220 sec for T_c, T_2, T_p, and T_1, respectively. From a previous investigation[9] concerning the energy transfer between the different spin systems in a similar ruby sample, we estimated $T_{ss,\mathrm{Al}}$ as being of the order of 1 sec.

Since T_c is by far the shortest time, the resonance circuit responds promptly to a transverse component of the magnetization. If we start from an inverted state to which a negative spin temperature θ_s or an equilibrium magnetization $M_z(0) = -M_0$ can be assigned, and if we restrict our consideration to the short-time regime $0 < t \ll T_{ss,\mathrm{Al}} < T_p, T_1$, we can write two nonlinear differential equations (in SI units) for the compo-

nents M_z' and M_v' of the fictitious magnetization in the longitudinal and transverse direction of the rotating frame of reference:

$$dM_v'/dt = \gamma M_z' B_1' - M_v'/T_2,$$

$$dM_z'/dt = -\gamma M_v' B_1'.$$

Here we assumed that ω_c is equal to the spin precission frequency ω_0 of the tuned NMR transition. B_1' is the fictitious rotating field induced by the true, transverse magnetization M_v inside the resonance coil.

For the central $(\frac{1}{2}, -\frac{1}{2})$ line in particular, where matrix-element considerations lead to $M_z = M_z'$, $M_v = 3M_v'$, and $B_1' = 3B_1$, we have $B_1 = \frac{9}{2}\mu_0\eta Q M_v$ (η being the filling factor). Thus, for the short-time regime, the equations of motion for the true components of the magnetization become

$$dM_v/dt = -\tfrac{9}{2}\mu_0\gamma\eta Q M_z M_v - M_v/T_2, \quad (1)$$

$$dM_z/dt = \tfrac{1}{2}\mu_0\gamma\eta Q M_v^2, \quad (2)$$

with the initial conditions $M_z(0) = -M_0$. They can readily be extended to the long-time regime when terms corresponding to $T_{ss,\mathrm{Al}}$, T_p, and T_1 are added. The condition for superradiance of the central line can be obtained from Eq. (1). If we set $M_0 = f(\theta_s)$ and define the radiation damping time as

$$T_R = 2/9\mu_0\gamma\eta Q M_0, \quad (3)$$

we must have $T_R \leq T_R{}^{\mathrm{th}} = T_2$, where $T_R{}^{\mathrm{th}}$ is the threshold value and $M_0{}^{\mathrm{th}}$ the corresponding magnetization of the two-level system. Since M_0 is related by the Boltzmann law to the spin temperature, $\theta_s{}^{\mathrm{th}}$ can be calculated.

In a first experiment the LC circuit was tuned consecutively to each of the five ^{27}Al transitions. The output of the resonant circuit was monitored for different amounts of microwave power delivered to the cavity. With a nagative nuclear-spin polarization and above a certain pump rate, cw self-oscillations were observed for the $(\frac{1}{2}, -\frac{1}{2})$ and the $(-\frac{3}{2}, -\frac{1}{2})$ transitions, whereas no maser oscillations were found for the other satellites even at the lowest attainable spin temperature $\theta_s{}^{\mathrm{min}} = -6$ mK. For the central line, as shown in Fig. 1, the cw maser output is plotted versus the supplied microwave power. The threshold values, $M_0{}^{\mathrm{th}} = 2.4$ A/m and $\theta_s{}^{\mathrm{th}} = -7$ mK, could be estimated from the measured DNP enhancement curve of a smaller specimen (thus avoiding nonlinear effects in the detector). With the experimental $Q = 40$ and $\eta = 0.85$, Eq. (3) leads to $T_R{}^{\mathrm{th}} = 3.5\times10^{-5}$ sec which has to be compared with the expected value $T_2 = 3.1\times10^{-5}$ sec, as obtained from the NMR linewidth. By use of Eq. (3) for the central line and properly modified expressions for the satellites, we calculated T_R for all five $\Delta m = \pm 1$ transitions at the minimum spin temperature $\theta_s{}^{\mathrm{min}} = -6$ mK reached in our experiments. If compared with the corresponding threshold values, $T_R{}^{\mathrm{th}} = T_2$, it is evident from Table I that only two lines are maser active, as in fact was observed.

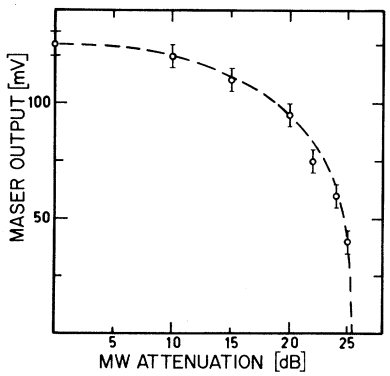

FIG. 1. Steady-state maser level (peak to peak) for the $(\frac{1}{2}, -\frac{1}{2})$ transition as a function of the microwave pumping power (100 mW at 0 dB).

In a second experiment the ^{27}Al system was cooled to $\theta_s{}^{\mathrm{min}}$ while keeping the LC circuit off-resonance. With an appropriate voltage step to the Varicap, the coil could be tuned selectively to one of the two maser-active lines. Figure 2 shows the output signal of the $(\frac{1}{2}, -\frac{1}{2})$ transition in a time interval of the order of $T_{ss,\mathrm{Al}}$. This response is typical and practically the same with or without the microwave pump on. Note, firstly, the large and sharp pulse shortly after the tuning has been performed; secondly, the transformation of the spiking maser pulses into a damped, sinusoidal relaxation oscillation[10]; and thirdly, the quasistationary oscillation with a peak-to-

TABLE I. Magnitude M_0 of the inverted magnetization at $\theta_s{}^{\mathrm{min}} = -6$ mK, and comparison of the radiation damping time T_R with the threshold value $T_R{}^{\mathrm{th}} = T_2$ for the five ^{27}Al $\Delta m = \pm 1$ transitions.

Transition	M_0 (A/m)	T_R (μsec)	T_2 (μsec)
$-5/2 \leftrightarrow -3/2$	3.47	38.5	27.2
$-3/2 \leftrightarrow -1/2$	3.12	26.8	28.8
$-1/2 \leftrightarrow +1/2$	2.8	26.5	30.6
$+1/2 \leftrightarrow +3/2$	2.53	33.2	27.2
$+3/2 \leftrightarrow +5/2$	2.28	58.8	27.2

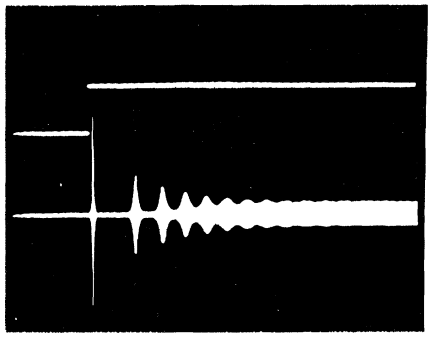

FIG. 2. Oscilloscope photograph showing the voltage step applied to the Varicap for tuning and the subsequent transient response of the $(\frac{1}{2},-\frac{1}{2})$ maser transition. The first pulse is clipped by the oscilloscope probe. The time between the first two bursts is approximately 100 msec.

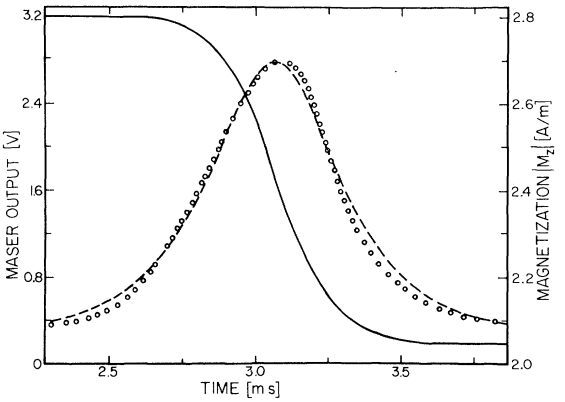

FIG. 3. Experimental (circles) and computed (dashed line) maser output voltage and computed z component $|M_z|$ (solid line) of the magnetization for the first superradiant pulse after tuning to the $(\frac{1}{2},-\frac{1}{2})$ transition.

peak voltage of 150 mV. For longer times, $t > T_{ss,\mathrm{Al}}$, with the microwave pump on, the maser output decreases to a constant value of 100 mV, typically. With the pump off, the signal decays to zero in a time of the order of 10 sec. From this behavior it is clear that the nonresonant two-level systems of ^{27}Al play the role of an intermediate reservoir of considerable heat capacity. This reservoir supplies spin energy via Cr^{3+} dipole-dipole interactions to the maser-active system and compensates for the losses in the LC circuit.

For a quantitive analysis of the supperradiant bursts, the first pulse was investigated separately. Starting from an inverted state with $\theta_s^{\min} = -6$ mK or $M_0 = 2.8$ A/m, a signal amplitude was observed as indicated by the circles in Fig. 3. After tuning the LC circuit, the pulse reaches a maximum of 2.7 V in a time of the order of 10^{-3} sec, depending on the initial conditions. The width at half-maximum is 5×10^{-4} sec. Both times are short with respect to $T_{ss,\mathrm{Al}}$. If we assume a small transverse component of the magnetization to be present in the initial state, we find that the shape of the pulse depends only, but critically, on the parameters η, M_0, T_2, and, as far as the pulse height is concerned, on the dimensions of the inductance coil. Using the experimental values as given before, Eqs. (1) and (2) were integrated. The computer solutions $V^c \sim M_v^c$, and M_z^c are shown in Fig. 3. It is evident that our model, with $\eta = 0.85$ as the only adjustable parameter, leads to a quantitative description of the superradiant burst. In addition, M_z^c indicates that the radiant two-level system ends in an inverted state with the magnetization $M_e = 2.05$ A/m such that $M_0^{\mathrm{th}} = \frac{1}{2}(M_0 + M_e) = 2.4$ A/m (a result which is anticipated from the analysis of giant laser pulses[11]). From here on, energy of the intermediate heat reservoir flows into the depleted system, which is pumped back above threshold, ready for a second oscillation burst, smaller but wider (Fig. 2).

In a final experiment, the LC circuit was tuned consecutively to both maser-active transitions. For each tuning only the first burst was recorded. If the time inverval τ between the tuning steps was kept short with respect to $T_{ss,\mathrm{Al}}$, an amplified and narrowed second pulse was observed as depicted in Fig. 4. Its shape follows again from Eqs. (1) and (2). The amplification is a direct consequence of the reduction of M_z for the first two-level system during its oscillation which, in turn, leads to an increase of the initial value of M_0 for the second one. By such consecutive tuning it is also possible to produce pulses

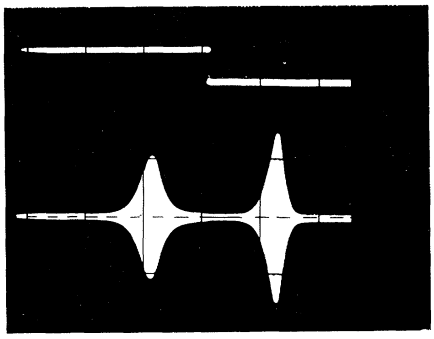

FIG. 4. Oscilloscope photograph showing the voltage steps applied to the Varicap for consecutive tuning to the $(\frac{1}{2},-\frac{1}{2})$ and $(-\frac{3}{2},-\frac{1}{2})$ transitions, and the shape of the respective output pulses ($\tau = 4.5$ msec).

from the maser-inactive lines.

In conclusion we may say that the oscillation pattern of such a Q-switched nuclear-spin-flip maser, due to its clearly resolved structure, contains valuable information concerning the spin dynamics of the sample which can be quantitatively accounted for. Thus, a maser of this sort must be considered as a new tool to study the energy transfer within complex spin systems at low temperature.

We gratefully acknowledge the stimulating discussions with B. Derighetti, P. Meier, and R. Pixley as well as the financial support of the Swiss National Science Foundation.

[1]J. Combrisson, A. Honig, and C. H. Townes, C. R. Acad. Sci. 242, 2451 (1956).

[2]A. Abragam, J. Combrisson, and I. Solomon, C. R. Acad. Sci. 245, 157 (1957).

[3]J. P. Wolfe and A. R. King, Chem. Phys. Lett. 40 451 (1976).

[4]E. Hundt, thesis, Universität Zürich, 1972 (unpublished).

[5]A. Abragam, *The Principles of Nuclear Magnetism* (Oxford Univ. Press, Oxford, England, 1970), p. 36 ff.

[6]N. Bloembergen and R. V. Pound, Phys. Rev. 95, 8 (1954).

[7]G. Feher, J. P. Gordon, E. Buehler, E. A. Gere, and C. D. Thurmond, Phys. Rev. 109, 221 (1958).

[8]A. Yariv, J. Appl. Phys. 31, 740 (1960).

[9]P. Bösiger, E. Brun, and D. Meier, in Proceedings of the Nineteenth Congress Ampere, Heidelberg, 1976 (to be published).

[10]A. Yariv, *Quantum Electronics* (Wiley, New York, 1975), p. 275.

[11]W. G. Wagner and B. A. Lengyel, J. Appl. Phys. 34, 2040 (1963).

Hydrodynamics of ^{3}He-A with Arbitrary Textures

Chia-Ren Hu* and Wayne M. Saslow
Department of Physics, Texas A & M University, College Station, Texas 77843
(Received 10 December 1976)

The general condition that determines the equilibrium textures of superfluid ^{3}He-A, incorporating the interdependence of $\vec{v}^{(s)}$, l_i, and $\partial_i l_j$, is derived. This condition is used to generalize Graham's hydrodynamics to allow for arbitrary equilibrium textures and steady-state flow. A new procedure is introduced to ensure that angular momentum is locally conserved; it is found to imply various relations between certain reaction coefficients.

It is now widely accepted that the orbital part of the order parameter of superfluid ^{3}He-A is a complex vector $\vec{\Delta} = \Delta_0(\hat{m} + i\hat{n})$, with $\hat{m}$, $\hat{n}$, and $\hat{l} \equiv \hat{m} \times \hat{n}$ forming a triad of three real, orthogonal unit vectors.[1] The vector $\hat{l}$ is called the orbital or anisotropy axis, and its space dependence in equilibrium defines the texture of the system. Ambegaokar, de Gennes, and Rainer[2] have shown that the vector $\hat{l}$ tends to be anchored normal to a wall. This has the important consequence that in any closed container, the texture of ^{3}He-A must be nonuniform. On the one hand, this nonuniformity makes the system more difficult to analyze; on the other hand, once nonuniform textures can be treated theoretically, it becomes possible to learn a great deal more about ^{3}He-A. From the theoretical studies of nonuniform textures which have been made so far,[3,4] one can conclude that appropriate measurements should yield new information about ^{3}He-A. Since various measurements on the hydrodynamic behavior of ^{3}He-A are currently being made employing various cell geometries,[5] there is a clear need for a general hydrodynamic theory with which to interpret such measurements.

Although Graham[6] has already developed a hydrodynamic theory of ^{3}He-A, his work applies only to a uniform texture with no steady-state flow. It is the purpose of the present work to derive the hydrodynamics for arbitrary textures, including nonlinear effects due to steady-state flow, and incorporating the interdependence of the superfluid velocity $\vec{v}^{(s)}$ with l_i and $\partial_i l_j$.[3] In the course of this work, the general condition for determining the equilibrium textures is obtained. It leads to a proper choice of variables in terms of which the general hydrodynamic equations are derived. A new procedure is then employed to enforce local conservation of angular momentum. We believe this procedure is more straightforward to follow than the existing one,[7,8] and should be generally applicable to other systems. Because this work is not restricted to uniform systems, many new reactive and dissipative terms

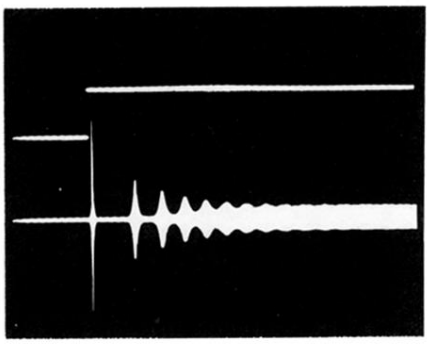

FIG. 2. Oscilloscope photograph showing the voltage step applied to the Varicap for tuning and the subsequent transient response of the $(\frac{1}{2}, -\frac{1}{2})$ maser transition. The first pulse is clipped by the oscilloscope probe. The time between the first two bursts is approximately 100 msec.

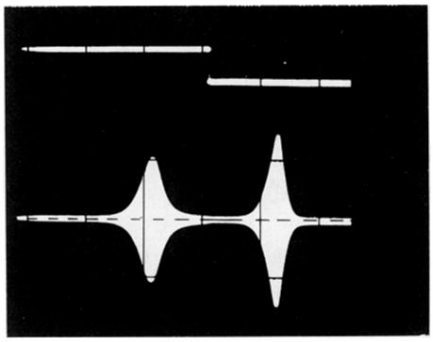

FIG. 4. Oscilloscope photograph showing the voltage steps applied to the Varicap for consecutive tuning to the $(\frac{1}{2},-\frac{1}{2})$ and $(-\frac{3}{2},-\frac{1}{2})$ transitions, and the shape of the respective output pulses ($\tau = 4.5$ msec).